

Epitaxial Growth of Superconducting $\text{Ba}(\text{Fe}_{1-x}\text{Co}_x)_2\text{As}_2$ Thin Films on Technical Ion Beam Assisted Deposition MgO Substrates

Kazumasa Iida, Jens Hänisch, Sascha Trommler, Vladimir Matias¹, Silvia Haindl, Fritz Kurth, Irene Lucas del Pozo, Ruben Hühne, Martin Kizszun, Jan Engelmann, Ludwig Schultz, and Bernhard Holzapfel

Leibniz-Institut für Festkörper- und Werkstofforschung (IFW) Dresden, P. O. Box 270116, 01171 Dresden, Germany
¹Superconductivity Technology Center, Los Alamos National Laboratory, Los Alamos, NM 87545, U.S.A.

The biaxially textured growth of superconducting Co-doped BaFe_2As_2 (Ba-122) thin films has been realized on ion beam assisted deposition (IBAD) MgO coated conductor templates by employing an iron buffer architecture. The iron pnictide coated conductor showed a superconducting transition temperature of 21.5 K, which is slightly lower than that of Co-doped Ba-122 films on single crystalline MgO substrates. A self-field critical current density of over $10^5 \text{ A}\cdot\text{cm}^{-2}$ has already been achieved even at 8 K. The current experiment highlights the potential of possible coated conductor applications of the iron-based superconductors.

As recently demonstrated, the implementation of an Fe buffer layer is beneficial for epitaxial growth of Co-doped BaFe_2As_2 (Ba-122) thin films on MgO single crystalline substrates since the metallic bond between the Fe layer and the Co-doped Ba-122 takes place on the Fe sublayer within the FeAs tetrahedron.¹⁾ Furthermore, a small lattice mismatch of 2.3% is realized between the (001) surface plane of Fe, which is rotated 45° in-plane, and the Fe sublayer in the Co-doped Ba-122 unit cell. As a result, excellent superconducting properties have been realized in Fe/Ba-122 bilayer system.²⁾ This opens the opportunity to grow Co-doped Ba-122 films on technical substrates (e.g., Hastelloy), on which textured MgO templates are prepared by ion beam assisted deposition (IBAD).

IBAD offers biaxially textured buffer layers for epitaxial growth of functional materials, such as high- T_c superconducting $\text{YBa}_2\text{Cu}_3\text{O}_7$ (YBCO).³⁾ In particular, the IBAD-MgO templates on Hastelloy are used for the 2nd generation YBCO coated conductor as the texture nucleation offers significantly faster processing than that in the case of using other materials.⁴⁾ At low temperatures, Co-doped Ba-122 offered the opportunity of very high upper critical field in combination with a much lower anisotropy compared to YBCO, which is one of the advantages for coated conductor applications. However, the critical current density (J_c) values of Fe-based superconducting wires or tapes published to date are not practical level, showing typically less than $10^3 \text{ A}\cdot\text{cm}^{-2}$ even at low temperature.^{5,6)}

Similarly to YBCO, grain boundaries (GBs) with misorientation angles above 6° seriously reduce the critical current for Co-doped Ba-122.⁷⁾ The same strong weak-link behavior due to GBs has been reported in F-doped LaFeAsO polycrystalline thin films.⁸⁾ Hence, the current limiting effects across GBs in Fe-based superconductors have found a general consensus, necessitating biaxially textured growth to achieve high critical currents.

Here, we report on the crystalline quality and superconducting properties of Co-doped Ba-122 grown on IBAD-MgO Hastelloy, offering the possibility for coated conductor processing of the new Fe-based superconductors.

10 mm wide commercial Hastelloy C-276 tapes were

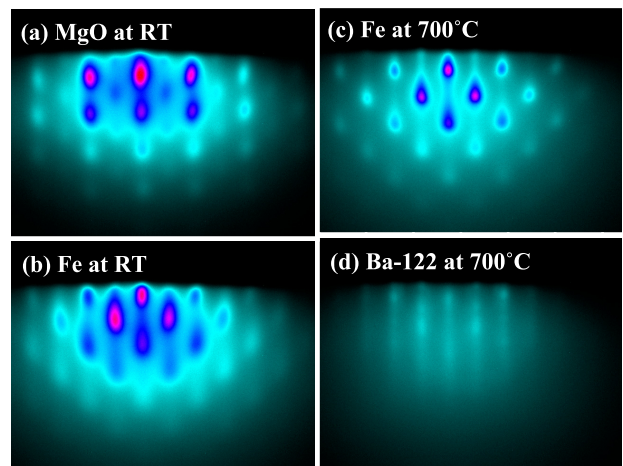


Fig. 1. (a) The RHEED image of an IBAD-MgO template at room temperature (RT) shows a good texture. The incident electron beam is parallel to [110] MgO. (b) Fe grows textured even at RT. (c) The crystalline quality improves at elevated temperatures. (d) Epitaxial growth of Co-doped Ba-122 on an Fe buffer layer.

planarized by solution planarization deposition (SDP) with 15 layers of Y_2O_3 with a total thickness of $1 \mu\text{m}$.⁹⁾ A roughness of around 0.6-0.8 nm on $5 \times 5 \mu\text{m}^2$ was achieved. The Y_2O_3 layer does not only provide a smooth and amorphous surface needed for IBAD but also protects the Ba-122 phase against detrimental diffusion of Ni and Cr from the Hastelloy tape. The IBAD-MgO layer, deposited at room temperature (RT), has a thickness of 5 nm and is covered by a homoepitaxial MgO layer of around 40 nm, which was deposited at 600°C [Fig. 1(a)]. More details of the template preparation can be found in ref. 10. For use in the pulsed laser deposition (PLD) system, the tape was mechanically cut into $10 \times 10 \text{ mm}^2$ pieces.

Fe layers of around 10 nm were deposited at RT on IBAD-MgO Hastelloy substrates by PLD, using a KrF excimer laser (248 nm) at a repetition rate of 8 Hz in an ultra high vacuum chamber (base pressure of 10^{-8} mbar). Reflection high-energy electron diffraction (RHEED) confirmed the epitaxial growth of Fe buffer layers even at RT [Fig. 1(b)], and their diffraction spots

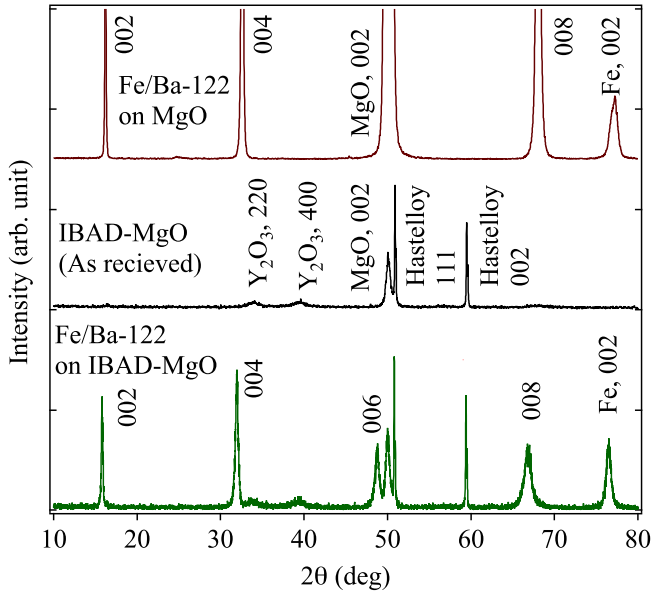


Fig. 2. The $\theta/2\theta$ -scans (Co- K_{α} radiation) of the Co-doped Ba-122 film on IBAD-MgO Hastelloy show a high phase purity and a c -axis texture (bottom traces). The data for Co-doped Ba-122 on a single crystalline MgO substrate and for bare IBAD-MgO Hastelloy are also plotted for clarity.

became sharper with increasing temperature as shown in Fig. 1(c), indicating that the crystalline quality improves. The Fe-covered IBAD-MgO Hastelloy substrate was then heated to 700°C for the deposition of about 50 nm thick Co-doped Ba-122 [Fig. 1(d)]. The detailed PLD target preparation and deposition conditions can be found in ref. 11.

Figure 2 exhibits the $\theta/2\theta$ -scans of the film on IBAD-MgO Hastelloy using Co- K_{α} radiation. All peaks were indexed with Co-doped Ba-122, Fe, Y_2O_3 , MgO and Hastelloy, indicating a high phase purity. Major peaks observed in Fig. 2 were the $00l$ reflection of the Co-doped Ba-122 and the 002 reflection of MgO together with Fe, implying that all deposited layers except Y_2O_3 were c -axis-oriented normal to the Hastelloy substrate plane. The Y_2O_3 peaks are due to a partial crystallization of the SDP Y_2O_3 layer during the deposition of the homoepitaxial MgO layer.

In order to confirm the epitaxial relation of the stacking layers for Co-doped Ba-122, Fe and MgO, pole figure measurements were conducted using Cu- K_{α} radiation. The respective contour plots in the logarithmic scale for the 103 reflection of Co-doped Ba-122, the 110 reflection of Fe, and the 220 reflection of MgO show a clear four-fold symmetry, indicating that all the layers grow epitaxially with the relation $(001)[100]$ Ba-122 $\parallel(001)[110]$ Fe $\parallel(001)[100]$ MgO [Fig. 3]. Table I shows a comparison of the crystalline quality between a film on IBAD-MgO and a Fe/Ba-122 bilayer on single crystalline MgO. The out-of-plane full width at half-maximum (FWHM) $\Delta\omega$, as well as the FWHM of the pole figures, $\Delta\phi$, of the Ba-122 film are similar to those of the underlying Fe layer. Therefore, in both cases, the texture is transferred to the superconducting Ba-122 layer. In contrast to Fe/Ba-122 bilayers on single crystalline MgO

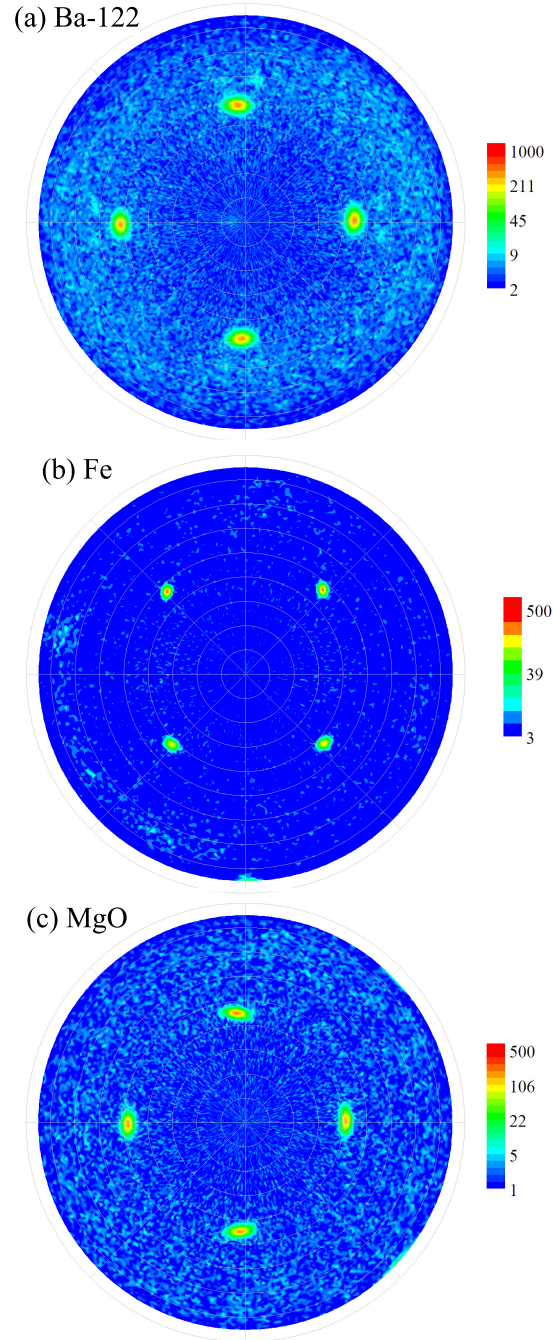


Fig. 3. (a) The 103 pole figure of Co-doped Ba-122 proves the in-plane texture. (b) Fe grows epitaxially on MgO with a 45° rotation. (c) MgO is biaxially textured on Y_2O_3 bed layered Hastelloy. The epitaxial relation is $(001)[100]$ Ba-122 $\parallel(001)[110]$ Fe $\parallel(001)[100]$ MgO.

substrates,¹⁾ the corresponding values are large, which is presumably due to the thin homoepitaxial layer of the IBAD-MgO templates. For the IBAD-MgO templates, the out-of-plane FWHM values of MgO reduce with increasing homo-epitaxial layer thickness and saturate of around 200 nm.¹⁰⁾ The in-plane texture shows the same tendency, but without saturation up to micrometer thicknesses. Hence, it might be possible to further improve the crystalline quality of the Fe buffer layer by employing

Table I. Average FWHM values of the ϕ -scans for MgO, Fe and Co-doped Ba-122 layers on IBAD-MgO Hastelloy. For comparison, the corresponding values on MgO single crystalline substrates are also shown. In both cases, the in-plane orientation of Co-doped Ba-122, $\Delta\phi_{\text{Ba-122}}$, is almost the same as that of Fe, $\Delta\phi_{\text{Fe}}$.

Substrates	$\Delta\phi_{\text{MgO}}$	$\Delta\phi_{\text{Fe}}$	$\Delta\phi_{\text{Ba-122}}$
IBAD-MgO Hastelloy	5.98°	4.71°	5.13°
MgO single crystal	0.58°	1.05°	0.95°

thicker IBAD-MgO templates, which leads to a higher degree of texture development in Co-doped Ba-122.

The normalized resistive traces of the Co-doped Ba-122 on IBAD-MgO Hastelloy are displayed in Fig. 4(a). The measurement was conducted using a physical property measurement system (PPMS; Quantum Design) with a standard four-probe method. The onset superconducting transition temperature T_c of the film on IBAD-MgO Hastelloy was around 21 K, which is slightly lower than that of the film on a MgO single crystalline substrate. As stated earlier, increased in-plane FWHM values indicate that GBs develop in the Co-doped Ba-122 layer, possibly leading to oxidation along the GBs, which would reduce T_c . In addition, the broad transition width of around 3 K may also be caused by the weak-link behavior. In YBCO, GBs reduce T_c even if they are not yet weak links (i.e., low-angle GBs) due to strain around the dislocation cores and the band bending effect. The same mechanisms might have a similar effect in the Co-doped Ba-122 film.

Albeit a relatively thick Y_2O_3 layer of 1 μm , an interdiffusion of Ni and Cr from Hastelloy to the superconducting layer cannot be ruled out completely due to the porous structures of these Y_2O_3 layers. Since both transition elements can enter the Fe site in the Ba-122 lattice, this diffusion would result in either electron or hole doping. The former induces superconductivity with a maximum T_c of 19 K,¹²⁾ and the latter does not show any signs of superconductivity at all.¹³⁾ Nevertheless, the T_c of the resultant film on IBAD-MgO Hastelloy decreased only by a small amount compared with that of fully optimized films on MgO single crystalline substrates.

Shown in Fig. 4(b) are $J_c - H$ characteristics for a Co-doped Ba-122 thin film on IBAD-MgO at 8 K. For these measurements, the films were cut into slabs measuring 1 mm in width and 8 mm in length with a wire saw. A criterion of 1 $\mu\text{V}\cdot\text{cm}^{-1}$ for evaluating J_c was employed. A self-field J_c of over $10^5 \text{ A}\cdot\text{cm}^{-2}$ has already been achieved even at 8 K. Further improvement in $J_c - H$ performance is possible since the fully optimized Fe/Ba-122 bilayers on MgO single crystalline substrates show one order of magnitude higher J_c values than that of the film of this study. The angular-dependent critical current density $J_c(\Theta)$ shown in Fig. 5 has a broad maximum at $\Theta = 90^\circ$, which arises from intrinsic pinning.¹⁴⁾

In summary, we have demonstrated the biaxially textured growth of superconducting Co-doped Ba-122 thin films on IBAD-MgO Hastelloy by employing an iron buffer layer architecture. The film on IBAD-MgO Hastelloy showed a superconducting transition temperature of 21 K with a large transition width of 3 K. A self-field J_c

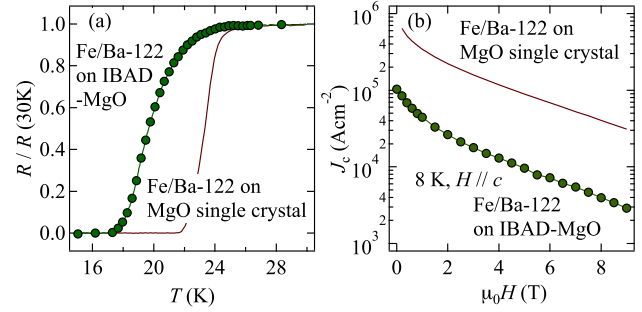


Fig. 4. (a) Normalized resistance of the Co-doped Ba-122 thin film on IBAD-MgO. The data were normalized to the value of 30 K. For comparison, the film on a MgO single crystalline substrate is also plotted. (b) $J_c - H$ characteristics for Co-doped Ba-122 thin film on IBAD-MgO at 8 K. A self-field J_c of over $10^5 \text{ A}\cdot\text{cm}^{-2}$ has been recorded.

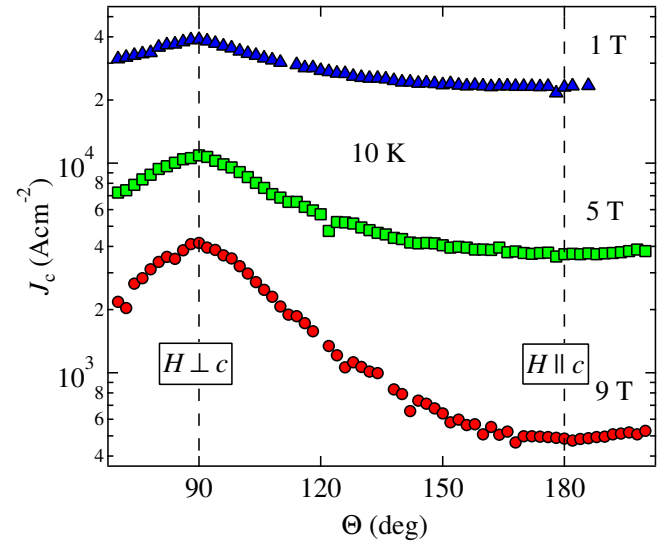


Fig. 5. Angular dependence of J_c for the Co-doped Ba-122 on IBAD-MgO substrates at 10 K under several magnetic fields. The magnetic field H was applied in the maximum Lorentz force configuration (H perpendicular to J) at an angle of Θ measured from the c -axis.

of over $10^5 \text{ A}\cdot\text{cm}^{-2}$ has already been achieved even at 8 K. These results open the avenue to the possibility of coated conductor growth of the new iron pnictide superconductors.

Acknowledgement The authors thank M. Kühnel and U. Besold at Leibniz-Institut für Festkörper- und Werkstofforschung Dresden for their technical support. We also thank C. Sheehan at Los Alamos National Laboratory for supplying solution deposited substrates. This work was partially supported by the German Research Foundation.

- 1) T. Thersleff, K. Iida, S. Haindl, M. Kidszun, D. Pohl, A. Hartmann, F. Kurth, J. Hänisch, R. Hühne, B. Rellinghaus, L. Schultz, and B. Holzapfel: Appl. Phys. Lett. **97** (2010) 022506.
- 2) K. Iida, S. Haindl, T. Thersleff, J. Hänisch, F. Kurth, M. Kidszun, R. Hühne, I. Mönch, L. Schultz, B. Holzapfel, and R. Heller: Appl. Phys. Lett. **97** (2010) 172507.
- 3) Y. Iijima, N. Tanabe, O. Kohno, and Y. Ikeno: Appl. Phys. Lett. **60** (1992) 769.

- 4) C. P. Wang, K. B. Do, M. R. Beasley, T. H. Geballe, and R. H. Hammond: *Appl. Phys. Lett.* **71** (1997) 2955.
- 5) Z. Gao, L. Wang, Y. Qi, D. Wang, X. Zhang, and Y. Ma: *Supercond. Sci. Technol.* **21** (2008) 105024.
- 6) Y. Mizuguchi, K. Deguchi, S. Tsuda, T. Yamaguchi, H. Takeya, H. Kumakura, and Y. Takano: *Appl. Phys. Express* **2** (2009) 083004.
- 7) S. Lee, J. Jiang, J. D. Weiss, C. M. Folkman, C. W. Bark, C. Tarantini, A. Xu, D. Abraimov, A. Polyanskii, C. T. Nelson, Y. Zhang, S. H. Baek, H. W. Jang, A. Yamamoto, F. Kametani, X. Q. Pan, E. E. Hellstrom, A. Gurevich, C. B. Eom, and D. C. Larbalestier: *Appl. Phys. Lett.* **95** (2009) 212505.
- 8) S. Haindl, M. Kidszun, A. Kauffmann, K. Nenkov, N. Kozlova, J. Freudenberger, T. Thersleff, J. Hänisch, J. Werner, E. Reich, L. Schultz, and B. Holzapfel: *Phys. Rev. Lett.* **104** (2010) 077001.
- 9) C. Sheehan, Y. Jung, T. Holesinger, D. M. Feldmann, V. Matias, C. Edney, J. F. Ihlefeld, and P. G. Clem: to be published in *Appl. Phys. Lett.*
- 10) V. Matias, J. Hänisch, E. J. Rowley, and K. Güth: *J. Mater. Res.* **24** (2009) 125.
- 11) K. Iida, J. Hänisch, R. Hühne, F. Kurth, M. Kidszun, S. Haindl, J. Werner, L. Schultz, and B. Holzapfel: *Appl. Phys. Lett.* **95** (2009) 192501.
- 12) N. Ni, A. Thaler, J. Q. Yan, A. Kracher, E. Colombier, S. L. Bud'ko, and P. C. Canfield: *Phys. Rev. B* **82** (2010) 024519.
- 13) A. S. Sefat, D. J. Singh, L. H. VanBebber, Y. Mozharivskyj, M. A. McGuire, R. Jin, B. C. Sales, V. Keppens, and D. Mandrus: *Phys. Rev. B* **79** (2009) 224524.
- 14) K. Iida, J. Hänisch, T. Thersleff, F. Kurth, M. Kidszun, S. Haindl, R. Hühne, L. Schultz, and B. Holzapfel: *Phys. Rev. B* **81** (2010) 100507(R).